Article

Design of an Azopolymer for Photo-Switchable Adhesive Applications

David Siniscalco [1,2], Laurence Pessoni [3], Anne Boussonnière [1], Anne-Sophie Castanet [1], Laurent Billon [3], Guillaume Vignaud [4] and Nicolas Delorme [1,*]

1 Institut des Molécules et Matériaux du Mans (IMMM), UMR CNRS 6283, Le Mans Université, Avenue Olivier Messiaen, 72000 Le Mans, France; david.siniscalco@univ-lemans.fr or dsiniscalco@ismans.cesi.fr (D.S.); anne.boussonniere@univ-lemans.fr (A.B.); anne-sophie.castanet@univ-lemans.fr (A.-S.C.)

2 Institut Supérieur des Matériaux et Mécaniques Avancées du Mans (ISMANS Groupe CESI), LINEACT, 44 avenue Frédéric Auguste Bartholdi, 72000 Le Mans, France

3 Bio-Inspired Materials Group—Functionalities & Self-Assembly, Université de Pau et des Pays de l'Adour, E2S UPPA, IPREM UMR 5254, 2 Avenue Angot, 64000 Pau, France; laurence.pessoni@univ-pau.fr (L.P.); billon@univ-pau.fr (L.B.)

4 IRDL, UMR CNRS 6027, Université Bretagne Sud, 56100 Lorient, France; guillaume.vignaud@univ-ubs.fr

* Correspondence: nicolas.delorme@univ-lemans.fr

Abstract: Significant research endeavors have been devoted to developing adhesives with reversible switching capabilities, allowing them to activate adhesion in response to diverse environmental stimuli. Among these, photo-switchable adhesives stand out as particularly promising. The presence of a photo-reversible solid-to-liquid transition, characterized by a transition temperature (T_{SL}), in certain azobenzene-containing polymers offers a compelling avenue for creating such adhesives. The development of a method based on Atomic Force Microscopy to measure both the glass transition temperature (T_g) and T_{SL} provided an opportunity to investigate the impact of various structural parameters on the solid-to-liquid transition of azopolymers. Our findings revealed that increasing the molecular weight (Mn) from 3400 to 8100 g/mol needed to achieve a highly cohesive adhesive resulted in an elevation in T_{SL} (>10 °C), making the solid-to-liquid transition at room temperature more challenging. However, incorporating a highly flexible substituent at the para position of the azobenzene group proved effective in significantly reducing the T_{SL} value (from 42 °C to 0 °C). This approach allows for the creation of photo-switchable adhesives with intriguing properties. We believe that our results establish a pathway toward developing a robust room-temperature photo-switchable adhesive.

Keywords: adhesive; phase transition; smart coating; polymer; AFM; azobenzene; glass temperature transition

1. Introduction

While advancements in adhesion technology have been noticeable in recent decades, creating materials with on-demand stickiness continues to pose a challenge. Extensive research efforts have been dedicated to the creation of switchable adhesives featuring an adjustable and reversible bonding–debonding process that can be activated in response to various environmental stimuli [1]. Among them, light is regarded as a highly promising external stimulus due to its benefits, including athermal operation, precise control, and environmental friendliness. Despite advancements in switchable adhesives, enhancing adhesion strength and reusability remains a formidable challenge.

It is widely acknowledged that the three main properties for characterizing the nature of an adhesive are tack (initial adhesion), adhesion (interaction with the substrate), and cohesion (intermolecular interactions), which all depend on the thermo-mechanical properties of the polymeric material [2]. Consequently, opting for materials capable of controlled

solid–liquid phase transitions holds promise for the development of improved switchable adhesives. Because light can induce a reversible change in the mechanical properties of the material called a solid-to-liquid phase transition [3,4], azobenzene-functionalized polymers, the so-called azopolymers, generate a strong enthusiasm for elaboration of photo-switchable adhesives [1,5–13]. Until recently, the characterization of the photo-reversible solid-to-liquid transition of azopolymer was made in almost all situations in a qualitative way. Typically, optical microscopy was used for bulk materials [11,14,15]. While convenient, this method proves unsatisfactory for the precise determination of transition conditions [16]. In a recent article [17], we demonstrated for the first time that the photo-reversible solid-to-liquid transition can be characterized by a transition temperature (T_{SL}). By using a method based on Atomic Force Microscopy (AFM), this temperature can be accurately measured, allowing us to propose a mechanism for the photo-reversible solid-to-liquid transition.

In the present article, the AFM method is used to measure both T_{SL} and Tg on thin coatings composed of various azopolymer architectures. By correlating the T_{SL} value with the chemical structure of the azopolymer, we gain insights into the chemical parameters governing the photo-reversible solid–liquid transition. Based on these findings, the selection of an optimized azopolymer architecture for the formulation of a room-temperature photo-switchable adhesive is performed and its properties are tested.

2. Materials and Methods

2.1. Azopolymer Synthesis

To synthesize the different azopolymers, we used Nitroxide-Mediated Polymerization (NMP). All the azopolymers synthesis details and characterization can be found in [16]. Size exclusion chromatography was used in THF as an eluent to check the molecular weight and the dispersity values of polymers. The chemical formula of azopolymers based on acrylate or the methacrylate polymerizable group and their main properties are presented in Table 1. Number-average molar mass (Mn) was calculated from a calibration derived from polystyrene standards. All the synthesized polymers present a dispersity between 1.2 and 1.3. Once purified, the polymers were kept in the dark at a low temperature (3 °C).

Table 1. Structure of the azopolymers synthetized and considered in this study.

Formula	R$_1$	R$_2$	Name	Mn (g/mol)	DP[1]	Conversion (%)
	C$_6$H$_{12}$	CH$_3$	P6-azo-CH3	3400	7	93
				4900	10	96
				5900	16	96
				8100	27	95
	C$_{10}$H$_{20}$	CH$_3$	P10-azo-CH3	6000	10	92
				11,400	27	97
	C$_6$H$_{12}$	C$_6$H$_{13}$	P6-azo-C6H13	7100	10	100
	C$_6$H$_{12}$	O-C$_6$H$_{13}$	P6-azo-OC6H13	7400	10	100

2.2. Azopolymer Coating

Azopolymer coatings were applied onto a meticulously cleaned microscopic glass slide. The cleaning procedure involved immersing the slide in a mixture of methanol and hydrochloric acid (in an equal volume ratio) for 30 min. Subsequently, the glass was thoroughly rinsed with ultrapure water, dried, and subjected to a 15-min treatment in a UV-ozone cleaner (Novascan PSD-UVT, Ames, IA, USA). For film preparation, a 10 g/L solution of azopolymer in dichloromethane (CH_2Cl_2) was slowly deposited onto a heated plate at 40 °C. The resulting films are homogeneous (Supplementary Figure S1) with a thickness ranging from 1 to 1.2 μm and an RMS roughness of 10 to 20 nm, as measured by AFM.

2.3. Atomic Force Microscopy (AFM)

AFM measurements were conducted using an Agilent 5500 equipped with an environmental chamber. Temperature control was achieved using a PID controller (Lakeshore-Westerville, OH, USA) coupled with a heating plate. Experiments covered a temperature ranging from −20 °C to 200 °C with an accuracy of 0.1 °C, facilitated by a Peltier and a heater stage. Stage temperature calibration was performed using different standard fusion point solids to cover the experimental temperature range. Force–distance measurements were obtained using CP-FM-SiO-B tips (NanoandMore, Paris, France) featuring a silica sphere (R = 3.5 μm). The spring constant, ranging from 0.5 to 1.2 N.m^{-1}, depending on the tip, was determined using the thermal noise method. A calibrated z-close loop scanner (90×90 μm^2) controlled the indentation depth and maximum load on films to prevent any deterioration. For each temperature, a 4×4 mapping on a 2×2 μm^2 surface was generated, with each pixel averaging 10 force-distance curves acquired at 1 Hz. Pull-off force intensities, Young moduli (JKR model, Poisson ratio of 0.33), and uncertainties were extracted from these measurements using Atomic J [18]. Relative pull-off force was calculated by dividing all the pull-off forces by the minimum pull-off force value.

2.4. Ellipsometry

Ellipsometry measurements were carried out using a Horiba spectroscopic ellipsometer. This instrument consists of a xenon source covering a wide spectral range from far infrared to ultraviolet (250–1700 nm), as well as a polarizer, an analyzer, and a monochromator responsible for managing dispersion and selecting wavelengths for a photomultiplier. The ellipsometer was equipped with a heating plate (LinKAM®TMS600—London, UK) to control thermal variations (30–145 °C) and transitions in the azopolymer films. Measurements for each sample were taken at 3 °C intervals between 25 and 106 °C, preceded by a 2-min equilibration period at a fixed temperature. The heating rate between the two measurements was set at 1°/min. To confirm the reproducibility of the measurements, at least three measurements were carried out on several samples. The thermal transitions of the trans isomer were assessed by introducing a UV filter (Longpass OD4—Edmund Optics, Villeurbane, France) that blocks UV radiation below 400 nm from the incident beam. This precautionary measure was taken to avoid any bias toward the cis state of the azopolymer. To analyze ellipsometry measurements, it is normally necessary to define a model representing the internal structure of the film in order to fit the curves. The limitations of this approach are that it can be difficult to define the most appropriate model, for example, the number of layers needed to perfectly describe the film morphology, etc. The choice of model can influence the adjustments and, therefore, the results obtained. Another analysis method [19] consists of observing the behavior of the raw data as a function of temperature, without modeling and adjustment. In this way, it is possible to detect transitions that would be less visible by choosing a model.

2.5. Adhesion Strength Measurement

Initially, two polycarbonate (PC) substrates, measuring 20 mm in length, 10 mm in width, and 3 mm in thickness, were manually polished for 15 s using 400 mesh sandpapers

(resulting in RMS roughness = 100 nm). Subsequently, they were washed with ethanol and allowed to air dry. Next, approximately 1–2 mg of the selected azopolymer was placed on the rough surface of one PC substrate, followed by exposure to UV irradiation for 30 s (365 nm, 300 mW.cm^{-2}). This UV treatment aimed to reach the T_{SL} of the azopolymer, ensuring it became fully molten. Afterward, another rough-surfaced PC substrate was manually pressed onto the molten azopolymer for 30 s. Upon cooling to room temperature, an azopolymer specimen was obtained with an approximate bonding area of 100 mm^2. Subsequently, the specimen was affixed to the grips of a universal tensile test machine (Mecmesin$^{®-}$, London, UK) and subjected to stretching at a rate of 2 mm.min^{-1} to generate the force–elongation curve [9].

2.6. Reversible Bonding–Debonding Experiment

Polyethylene Naphthalate (PEN), Polycarbonate (PC), and Polyethylene Terephthalate (PET) strips with dimensions of 10 cm (length) × 5 mm (width) × 0.3 mm (thickness) were used. First, 1–2 mg of azopolymer was placed on one end of the strip. After 2 min of UV irradiation, the azopolymer was molten and was then glued (by thumb pressure for 30 s) with the other end of the stripe to acquire a ring. The ring was again submitted to UV light (365 nm, 300 mW.cm^{-2}) for the debonding process [9].

3. Results

3.1. Measurement of T_g and T_{SL}

The comprehensive experimental methodology for measuring T_{SL} on the azopolymer coating has been thoroughly elucidated in earlier publications [17,20]. In summary, by performing pull-off force measurement between the AFM tip and the surface of an azopolymer coating as a function of the film temperature, different transition temperatures can be detected. As seen in Figure 1a for P6-azo-CH3 azopolymer (Mn = 8100 g/mol), the glass temperature transition (T_g) for both trans (T_g(trans) = 54(2) °C) and cis (T_g(cis) = 32(2) °C) isomers are identified as the first slope breakage of the pull-off force vs. the temperature curve. We also demonstrated in our previous articles that the position of the maximum pull-off force (i.e., T_{max}) corresponds to a solid-like to liquid-like transition [17,20]. For P6-azo-CH3 azopolymer with Mn = 8100 g/mol, we measured T_{max}(trans) = 90(2)° and T_{max}(cis) = 42(2) °C. All these temperature transitions were also detected on azopolymer coatings by multiwavelength ellipsometry. Figure 1b shows the quantity I_S extracted from the output signal by harmonic analysis (synchronous detection at the modulator frequency) and related to the ellipsometric angles (ψ and Δ) by $I_s = \sin(2\psi)\sin(\Delta)$. Its behavior as a function of temperature is entirely consistent with the AFM measurements. These earlier investigations have contributed to the understanding of the photo-reversible solid-to-liquid transition mechanism. As shown in Figure 1b, the trans-to-cis isomerization of the azopolymer coating by UV irradiation (UV–visible spectra are provided in Supplementary Figure S2) is not sufficient to reach the solid-to-liquid transition. A greater irradiation intensity (or external heating) is required to surpass T_{max}(cis). Reversibility is achieved either through storage of the material in the dark or exposure to green light irradiation. Consequently, T_{SL} and T_{max}(cis) represent the same transition temperature [17]. With the ability to accurately measure T_g and T_{SL}, we are able to study the influence of the polymer architecture on the photo-reversible solid-to-liquid transition.
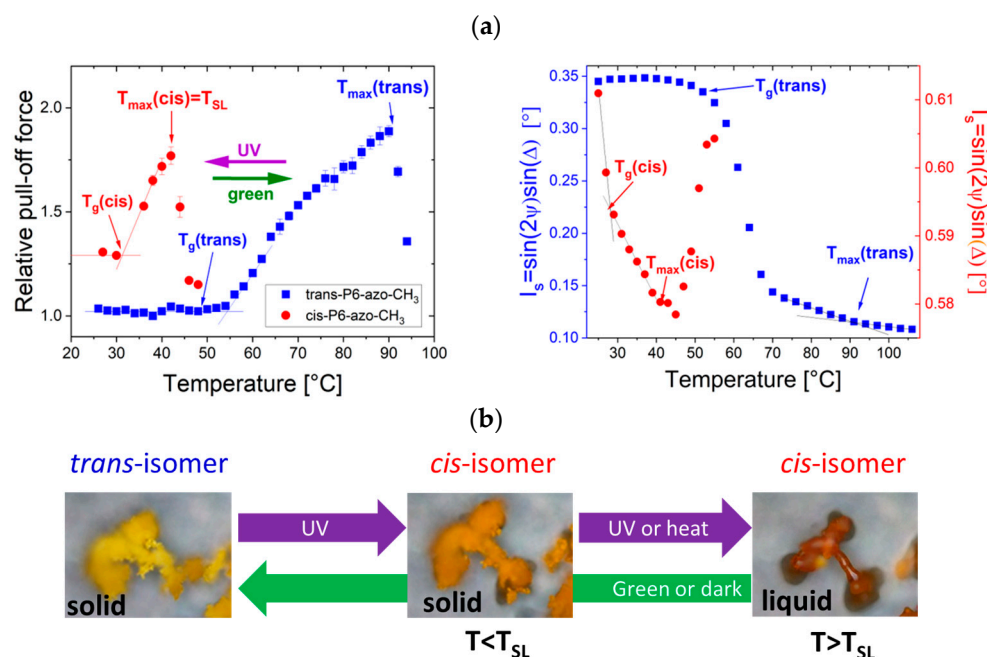
(a)

(b)

Figure 1. (**a**) (**left**) Relative pull-off force vs. the temperature curve and (**right**) raw ellipsometry data vs. temperature at an energy of 1.2 eV, for trans- and cis-P6-azo-CH3 (Mn = 8100 g/mol) (for the cis experiment, irradiation with a UV lamp: λ_{max} = 365 nm, E_e = 300 mW.cm^{-2}, t = 30 s). (**b**) Optical microscopy images (350 μm × 264 μm) of P6-azo-CH3 grains as a function of the irradiation and temperature conditions.

3.2. Influence of Azopolymer Chain Length

In 2020, Chen et al. synthesized azopolymers with the same chemical structure as P6-azo-CH3. They measured an increase in T_g(trans) from 48 to 80 °C for a molecular weight (Mn) from 5000 to 100,000 g/mol [21]. In this work, pull-off force vs. temperature experiments were performed on P6-azo-CH3 with Mn = 3400 to 8100 g/mol in order to measure the evolution of both T_g and T_{SL} with Mn. The extracted T_g and T_{SL} values from the pull-off force vs. temperature curves (Supplementary Figure S3) are plotted as a function of Mn in Figure 2. At first, it can be seen that T_g(trans) is always measured above T_g(cis). This may be explained by the conformation of the azomolecule substituent. Indeed, the trans-to-cis photo-isomerization leads to a modification of the geometry of the azomolecule substituent, which passes from a rod-like shape favoring good packing with adjacent azomolecules to a banana-like shape increasing the free volume of the polymer material. Although the measured T_g(trans) values of the P6-azo-CH3 azopolymers are in agreement with those measured by Chen et al. [21], here, we demonstrate that both T_g(trans) and T_g(cis) increase with Mn. This evolution, expected for linear polymers with low Mn, follows the Fox–Flory equation: $T_g = T_{g,\infty} - \frac{K}{Mn}$, where $T_{g,\infty}$ is a parameter that can be associated with the glass transition for an infinity high Mn and K is a material dependent parameter [22]. The fitting parameters are available in Supplementary Table S1 and show a similar K parameter (K~72,000–73,000 g/mol) for both the trans and cis isomers, which is closed from the calculated critical entanglement molecular weight (i.e., Mc = 68,000 g/mol) for this azopolymer [21]. Finally, we can observe that for this polymer architecture, whereas T_{max}(trans) increases with Mn, T_{SL} seems to saturate for Mn greater than 5000 g/mol. At present, the absence of theoretical work concerning the solid-to-liquid transition hinders drawing any definitive conclusions about this evolution.
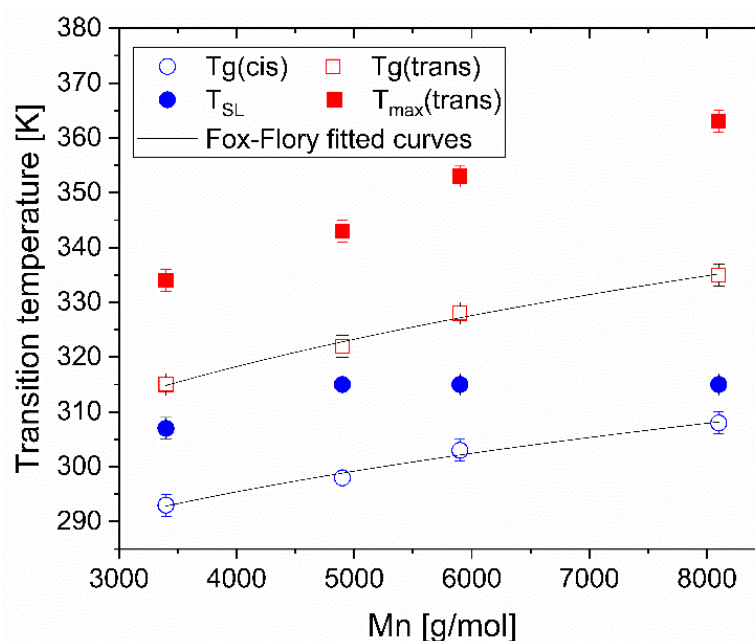
Figure 2. Evolution of Tg and T_{SL} measured by AFM for both the trans and cis isomers as a function of the molecular mass of the P6-azo-CH3 azopolymers.

3.3. Influence of the Alkyl Length Ligand

For acrylate azopolymers, Weiss et al. observed that the solid-to-liquid transition is impacted by the alkyl spacer length since the transition was only observed for *n* = 6 and n = 12 (with n the number of carbon atoms) [23]. Here, we compare azopolymers with alkyl spacer lengths of *n* = 6 (P6-azo-CH3) and *n* = 10 (P10-azo-CH3) with two different Mn (Supplementary Figure S4).

When comparing azopolymers with different linker lengths but similar Mn, it can be seen (Table 2) on one side that T_g(trans) and T_{max}(trans) are close and thus fairly impacted by the linker length. On the other side, an increase in the linker length leads to a strong decrease ($\Delta T < -20$ °C) of both T_g(cis) and T_{SL}. For a similar Mn (i.e., 8600 g/mol), Weis measured T_g(cis) = -14 °C on powder for the *n* = 12 linker [23], which is in agreement with the evolution observed here. These results may indicate that the linker length has a stronger impact on the thermo-mechanical properties of the cis form than on those of the trans form. The molecule packing of the trans rod-like shape azomolecule may be fairly impacted by the linker length, whereas in the cis conformation, the banana shape with a higher linker length may create a consequent excess of free volume and thus a strong decrease in the transition temperatures.

Table 2. Influence of the linker length on transition temperatures T_g and T_{max}. All the measured data have measurement uncertainties of 2 °C.

		Tg (°C)	**T_{max} (°C)**
P6-azo-CH3	Trans	52	80
Mn=5900 g/mol	Cis	30	42 (T_{SL})
P10-azo-CH3	Trans	52	75
Mn=6000 g/mol	Cis	0	15 (T_{SL})
P6-azo-CH3	Trans	54	90
Mn=8100 g/mol	Cis	32	42 (T_{SL})
P10-azo-CH3	Trans	60	85
Mn=11400 g/mol	Cis	47	60 (T_{SL})

3.4. Influence of the Substituent Nature

In order to study the influence of the azobenzene chemical structure, we compared the values of T_g and T_{SL} for three azopolymers, namely, (P6-azo-CH3, P6-azo-C6H13, and P6-azo-OC6H13) (Supplementary Figure S5). These azopolymers have similar Mn and the same alkyl linker length ($n = 6$) but a different substituent on the para position of the azobenzene group.

When comparing P6-azo-CH3 and P6-azo-C6H13 (Table 3), we can see that the increase in the alkyl tail of the substituent leads to a net decrease in all the transition temperatures. Our results agree with the work of Liang et al. [24], who measured T_g(trans) = 68 °C and T_g(cis) = −27 °C for $n = 10$, and with Li et al. [25], who studied the effect of substituents length on the transition temperature of alkyl on poly(n-alkyl-acrylate) polymer and demonstrated that T_g decreases with the substituent length, reflecting the greater side chain mobilities of long alkyl substituents.

Table 3. Influence of the substituent nature on the transition temperatures. All the measured data have measurement uncertainties of 2 °C.

		Tg (°C)	**Tmax (°C)**
P6-azo-CH3	Trans	54	90
Mn=8100 g/mol	Cis	32	42 (T_{SL})
P6-azo-C6H13	Trans	33	57
Mn=7100 g/mol	Cis	<−10	0 (T_{SL})
P6-azo-OC6H13	Trans	45	87
Mn=7400 g/mol	Cis	<20	30 (T_{SL})

Whereas P6-azo-C6H13 and P6-azo-OC6H13 have comparable substituent lengths, they show different behavior. Indeed, both the T_g and T_{max} transition temperatures of P6-azo-OC6H13 are much higher. Compared with P6-azo-C6H13, the presence of the oxygen group in P6-azo-OC6H13 may, via a mesomeric effect with the azobenzene group, lead to a higher rigidity of the substituent [26,27]. This loss of flexibility may explain the observed increase in both T_g and T_{max}. This outcome illustrates that the crucial factor in adjusting T_{SL} may not be the length of the substituent but rather its flexibility.

3.5. Photo-Switchable Adhesive

Hot melt adhesives (HMAs) are widely used in the industry because they are solvent-free, they form a strong bond quickly, simply by cooling, are compatible with most materials, and are clean and easy to handle [28]. Such adhesives undergo a phase transition into a liquid state when heated, facilitating their application between two substrates. Upon cooling, the adhesive solidifies via physical crosslinks and creates a bond between the substrates. For photo-switchable adhesives, the goal is to replace the heating/cooling step of the HMA with light irradiation. As a consequence, a good candidate should present (1) a temperature of solid–liquid transition (T_{SL}) slightly above the operating temperature. This is essential because, during the bonding process, the liquid form can be rapidly achieved using moderate UV irradiation. Subsequently, reversible debonding can be accomplished by UV irradiation of the assembly (cis liquid form and loss of adhesive cohesion). (2) The glass transition temperature of the trans state (T_g trans) should surpass the operating temperature, and (3) Mn should be high. These two last conditions ensure that after the bonding process, a solid form can be attained with thermal cis-to-trans isomerization and that physical crosslink may append both enhancing the cohesion of the adhesive. As a consequence, in order to prepare an adhesive with an operating temperature of 20 °C, the selected formulation should fulfill the following conditions: (1) $T_{SL} \leq 35$ °C; (2) T_g(trans) > 20 °C; and (3) high Mn. Even if high Mn azopolymers could not be obtained in this study, among the synthesized azopolymers, only two fulfill these conditions: P6-azo-C6H13 and P6-azo-OC6H13.

At first, the adhesion strengths were investigated by lap shear strength tests using polycarbonate substrates to determine the best adhesive candidate. The stress−strain curves of P6-azo-C6H13 and P6-azo-OC6H13 are shown in Figure 3. The bonding shear strengths of the two adhesives were 3.3 MPa and 6.1 MPa, respectively. Even though the absolute values of adhesive strength have to be taken with caution because they are related to the condition of the bonded substrate, the measured values are comparable with the ones measured by Lee et al. [8] and are higher than Li et al. [10,13]. It is clear that P6-azo-OC6H13 shows a higher adhesive strength than P6-azo-C6H13 in the trans state. This can be explained by the difference in T_g(trans). Indeed, the T_g(trans) of P6-azo-C6H13 is lower than the T_g(trans) of P6-azo-OC6H13 and much closer to the ambient temperature. As a result, the mechanical properties at 20 °C (i.e., modulus, cohesive energy...) of P6-azo-C6H13 are lower than P6-azo-OC6H13.
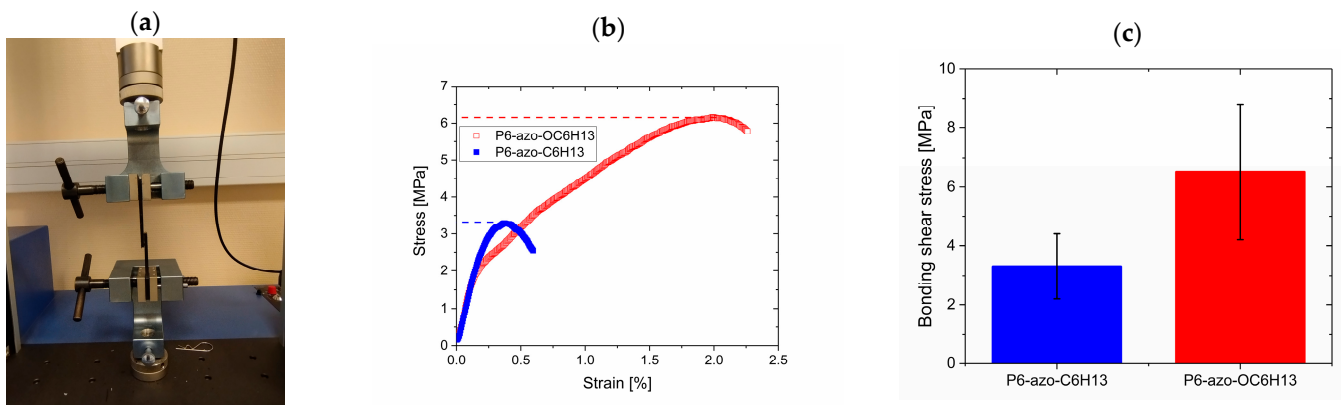
Figure 3. (**a**) Photograph of the shear lap test and examples of (**b**) the stress−strain curves and (**c**) bonding shear stress extracted from the stress–strain curves for P6-azo-C6H13 and P6-azo-OC6H13 glued on the PC substrate.

Based on the good adhesive strength of the two candidates, the reversible opening and closing of a plastic ring were successfully achieved (Figure 4) [9]. After the deposition of azopolymer powder on one end of the strip, the powder was UV irradiated for 30 s (365 nm, 100 mW.cm^{-2}) in order to cause the trans–cis isomerization and the reaching of T_{SL} where the solid-to-liquid transition occurs. The polymer strip was then pressed end-to-end under room light to acquire a ring. We checked that the pressing time of t = 30 s was enough for the back cis–trans isomerization to proceed. Debonding of the ring can be performed upon UV irradiation, where the ring opens within 30 s. The opening and closing of the ring could be reversibly achieved when the adhesive position was exposed to alternating UV and pressure. Different polymer film substrates were tested as a ring strip either with P6-azo-OC6H13 or P6-azo-C6H13 glue. To compare the different assemblies, the time for the ring to self-debond when kept at room temperature was measured. The results presented in Figure 4b show that whatever the substrate, P6-azo-OC6H13 is a stronger adhesive than P6-azo-C_6H_{13}, indicating that P6-azo-OC6H13 seems to be a good candidate for a photo-switchable adhesive.
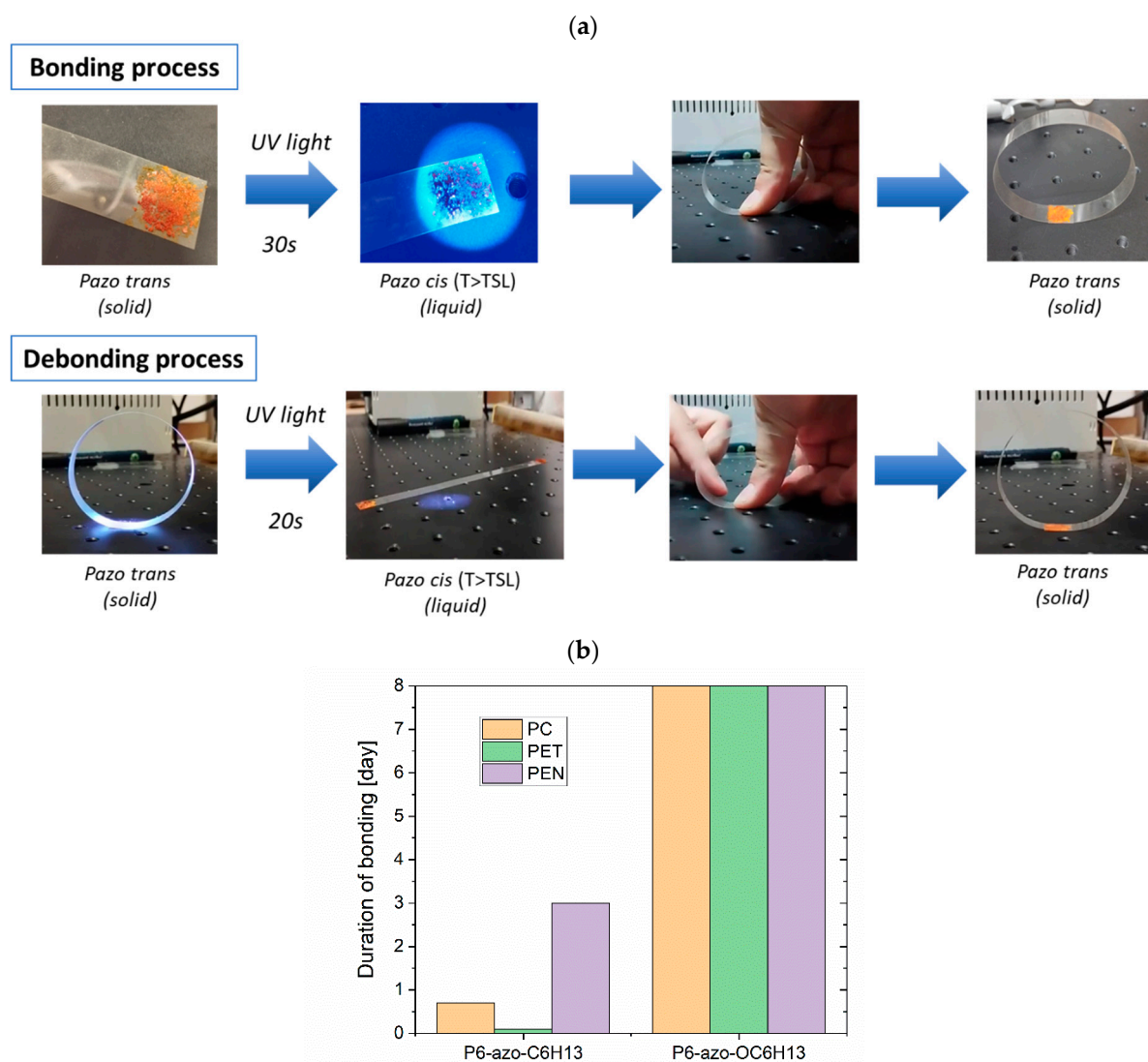
Figure 4. (**a**) Schematic illustration and photographs showing the light-induced reversible opening and closing of a polymer ring glued with the P6-azo-OC6H13 azopolymer. (**b**) Duration of bonding of the ring glued with either P6-azo-C6H13 or P6-azo-OC6H13 when rings are kept at room temperature for a total duration of 8 days.

4. Conclusions

In summary, the possibility of using the pull-off force vs. temperature method to measure both T_g and T_{SL} gave us the opportunity to study the effect of different structural parameters on the solid-to-liquid transition of azopolymers. Our study has demonstrated that the increase in Mn needed to have high cohesive adhesive led to an increase in T_{SL}, rendering the solid-to-liquid transition more difficult to access. However, the use of a highly flexible substituent on the para position of the azobenzene group gives the opportunity to strongly decrease the value of T_{SL} and obtain photo-switchable adhesives with interesting properties. Upon alternating UV light exposure, the adhesive showed reversible debonding and bonding, which was applicable to various substrates. The result indicates that P6-azo-OC6H13 had superior adhesive performance and reusability, which may be applicable in the near future. We believe that our results pave the way for the route toward a robust photo-switchable adhesive.

References

1. Liu, Z.; Yan, F. Switchable Adhesion: On-Demand Bonding and Debonding. *Adv. Sci.* **2022**, *9*, 2200264. [CrossRef] [PubMed]
2. Benedek, I. *Pressure-Sensitive Adhesives and Applications*; CRC Press: Boca Raton, FL, USA, 2004. [CrossRef]
3. Zhou, H.; Xue, C.; Weis, P.; Suzuki, Y.; Huang, S.; Koynov, K.; Auernhammer, G.K.; Berger, R.; Butt, H.-J. Photoswitching of glass transition temperatures of azobenzene-containing polymers induces reversible solid-to-liquid transitions. *Nat. Chem.* **2017**, *9*, 145–151. [CrossRef] [PubMed]
4. Ito, S.; Yamashita, A.; Akiyama, H.; Kihara, H.; Yoshida, M. Azobenzene-Based (Meth)acrylates: Controlled Radical Polymerization, Photoresponsive Solid–Liquid Phase Transition Behavior, and Application to Reworkable Adhesives. *Macromolecules* **2018**, *51*, 3243–3253. [CrossRef]
5. Akiyama, H.; Fukata, T.; Yamashita, A.; Yoshida, M.; Kihara, H. Reworkable adhesives composed of photoresponsive azobenzene polymer for glass substrates. *J. Adhes.* **2017**, *93*, 823–830. [CrossRef]
6. Ohzono, T.; Saed, M.O.; Terentjev, E.M. Enhanced Dynamic Adhesion in Nematic Liquid Crystal Elastomers. *Adv. Mater.* **2019**, *31*, 1902642. [CrossRef]
7. Koike, M.; Aizawa, M.; Minamikawa, H.; Shishido, A.; Yamamoto, T. Photohardenable Pressure-Sensitive Adhesives using Poly(methyl methacrylate) containing Liquid Crystal Plasticizers. *ACS Appl. Mater. Interfaces* **2021**, *13*, 39949–39956. [CrossRef]
8. Lee, T.-H.; Han, G.-Y.; Yi, M.-B.; Kim, H.-J.; Lee, J.-H.; Kim, S. Rapid Photoresponsive Switchable Pressure-Sensitive Adhesive Containing Azobenzene for the Mini-Light Emitting Diode Transfer Process. *ACS Appl. Mater. Interfaces* **2021**, *13*, 43364–43373. [CrossRef]
9. Zhang, P.; Cai, F.; Wang, W.; Wang, G.; Yu, H. Light-Switchable Adhesion of Azobenzene-Containing Siloxane-Based Tough Adhesive. *ACS Appl. Polym. Mater.* **2021**, *3*, 2325–2329. [CrossRef]
10. Imato, K.; Momota, K.; Kaneda, N.; Imae, I.; Ooyama, Y. Photoswitchable Adhesives of Spiropyran Polymers. *Chem. Mater.* **2022**, *34*, 8289–8296. [CrossRef]
11. Zhao, R.; Mu, J.; Bai, J.; Zhao, W.; Gong, P.; Chen, L.; Zhang, N.; Shang, X.; Liu, F.; Yan, S. Smart Responsive Azo-Copolymer with Photoliquefaction for Switchable Adhesive Application. *ACS Appl. Mater. Interfaces* **2022**, *14*, 16678–16686. [CrossRef]
12. Hu, J.; Song, T.; Yu, M.-M.; Yu, H. Optically Controlled Solid-to-Liquid Phase Transition Materials Based on Azo Compounds. *Chem. Mater.* **2023**, *35*, 4621–4648. [CrossRef]
13. Li, J.; Zhang, Q.-Y.; Lu, X.-B. Azopolyesters with Intrinsic Crystallinity and Photoswitchable Reversible Solid-to-Liquid Transitions. *Angew. Chem. Int. Ed.* **2023**, *62*, e202311158. [CrossRef] [PubMed]
14. Shang, C.; Xiong, Z.; Liu, S.; Yu, W. Molecular Dynamics of Azobenzene Polymer with Photoreversible Glass Transition. *Macromolecules* **2022**, *55*, 3711–3722. [CrossRef]

15. Yang, B.; Cai, F.; Huang, S.; Yu, H. Athermal and Soft Multi-Nanopatterning of Azopolymers: Phototunable Mechanical Properties. *Angew. Chem. Int. Ed.* **2020**, *59*, 4035–4042. [CrossRef] [PubMed]
16. Pessoni, L.; Siniscalco, D.; Boussonnière, A.; Castanet, A.-S.; Billon, L.; Delorme, N. Photo-reversible solid to liquid transition of azobenzene containing polymers: Impact of the chemical structure and chain length. *Eur. Polym. J.* **2022**, *174*, 111297. [CrossRef]
17. Siniscalco, D.; Pessoni, L.; Billon, L.; Boussonnière, A.; Castanet, A.-S.; Bardeau, J.-F.; Nickmilder, P.; Leclère, P.; Delorme, N. Measurement of the Transition Temperature Governing the Photoinduced Reversible Solid-to-Liquid Transition of Azobenzene-Containing Polymers. *ACS Appl. Polym. Mater.* **2023**, *5*, 7358–7363. [CrossRef]
18. Hermanowicz, P.; Sarna, M.; Burda, K.; Gabryś, H. AtomicJ: An open source software for analysis of force curves. *Rev. Sci. Instrum.* **2014**, *85*, 063703. [CrossRef]
19. El Ouakili, A.; Vignaud, G.; Balnois, E.; Bardeau, J.-F.; Grohens, Y. Multiple glass transition temperatures of polymer thin films as probed by multi-wavelength ellipsometry. *Thin Solid Film* **2011**, *519*, 2031–2036. [CrossRef]
20. Delorme, N.; Chebil, M.S.; Vignaud, G.; Le Houerou, V.; Bardeau, J.F.; Busselez, R.; Gibaud, A.; Grohens, Y. Experimental evidence of ultrathin polymer film stratification by AFM force spectroscopy. *Eur. Phys. J. E* **2015**, *38*, 56. [CrossRef]
21. Chen, M.; Yao, B.; Kappl, M.; Liu, S.; Yuan, J.; Berger, R.; Zhang, F.; Butt, H.-J.; Liu, Y.; Wu, S. Entangled Azobenzene-Containing Polymers with Photoinduced Reversible Solid-to-Liquid Transitions for Healable and Reprocessable Photoactuators. *Adv. Funct. Mater.* **2020**, *30*, 1906752. [CrossRef]
22. Fox, T.G.; Loshaek, S. Influence of molecular weight and degree of crosslinking on the specific volume and glass temperature of polymers. *J. Polym. Sci.* **1955**, *15*, 371–390. [CrossRef]
23. Weis, P.; Hess, A.; Kircher, G.; Huang, S.; Auernhammer, G.K.; Koynov, K.; Butt, H.-J.; Wu, S. Effects of Spacers on Photoinduced Reversible Solid-to-Liquid Transitions of Azobenzene-Containing Polymers. *Chem. Eur. J.* **2019**, *25*, 10946–10953. [CrossRef]
24. Liang, S.; Li, S.; Yuan, C.; Zhang, D.; Chen, J.; Wu, S. Polyacrylate Backbone Promotes Photoinduced Reversible Solid-To-Liquid Transitions of Azobenzene-Containing Polymers. *Macromolecules* **2023**, *56*, 448–456. [CrossRef]
25. Li, T.; Li, H.; Wang, H.; Lu, W.; Osa, M.; Wang, Y.; Mays, J.; Hong, K. Chain flexibility and glass transition temperatures of poly(n-alkyl (meth)acrylate)s: Implications of tacticity and chain dynamics. *Polymer* **2021**, *213*, 123207. [CrossRef]
26. Velde, C.V.; Bultinck, E.; Tersago, K.; Alsenoy, C.V.; Blockhuys, F. From anisole to 1,2,4,5-tetramethoxybenzene: Theoretical study of the factors that determine the conformation of methoxy groups on a benzene ring. *Int. J. Quantum Chem.* **2007**, *107*, 670–679. [CrossRef]
27. Arakawa, Y.; Ishida, Y.; Shiba, T.; Igawa, K.; Sasaki, S.; Tsuji, H. Effects of alkylthio groups on phase transitions of organic molecules and liquid crystals: A comparative study with alkyl and alkoxy groups. *CrystEngComm* **2022**, *24*, 1877–1890. [CrossRef]
28. Li, W.; Bouzidi, L.; Narine, S.S. Current Research and Development Status and Prospect of Hot-Melt Adhesives: A Review. *Ind. Eng. Chem. Res.* **2008**, *47*, 7524–7532. [CrossRef]